ISSN-1996-918X

Pak. J. Anal. Environ. Chem. Vol. 24, No. 1 (2023) 48 – 62

http://doi.org/10.21743/pjaec/2023.06.05

Seasonal and Spatial Characteristics of Suspended Sediment Load and their Controlling Factors in the Upper Indus River Basin, Pakistan

Muhammad Dodo Jagirani[1,2,3,4], XiaonanShi[1,2],Fan Zhang[1,2,3], Shahram Khalighi-Sigaroodi[1,6], Chen Zeng[1], Xiong Xiao[1,2], Li Wang[1,2], Faizan ur Rehman Qaiser[1,5], and GuanxingWang[1,2]

[1]Key *Laboratory of Tibetan Environment Changes and Land Surface Processes, Institute of Tibetan Plateau Research, Chinese Academy of Sciences, Beijing, China.*

[2]*University of Chinese Academy of Sciences, Beijing, China.*

[3]*CAS Center for Excellence in Tibetan Plateau Earth Sciences, Beijing, China.*

[4]*Department of Geography, Government Boys Degree College Qasimabad, Hyderabad, Sindh, Pakistan.*

[5]*Department of Earth Science, COMSATS University Abbottabad Campus, Pakistan.*

[6]*Faculty of Natural Resources, University of Tehran, Karaj, Iran.*

**Corresponding Author Email:mdjagirani@itpcas.ac.cn*

Received 14 November 2022, Revised 14 June 2023, Accepted 20 May 2023

Abstract

Understanding the seasonal and spatial characteristics of suspended sediment load is extremely important for efficient water resource management. The characteristics of suspended sediment load reflect the soil erosion, transport and deposition. The upper Indus basin is a single source of fresh water and hydropower generation for the surroundings and downstream areas with a population of millions approximately. Simultaneously, the water resources in this area are badly affected by the sedimentation. Therefore, the focus of this study is to evaluate the seasonal variation and spatial distribution of suspended sediment load and figure out their controlling factors by using hydrometeorological data series collected from WAPDA and PMD. Annual sediment load at four mainstream stationsaccounted for 34.0 at Kachura, 86.7 at Bunji Bridge, 75.7 at Shatial and 57.7 (Mt) at Besham Qila, respectively. The high sediment loads were observed during the summer season, accounting for 77.4% at Kachura, 85.6% at Bunji Bridge, 73.7% at Shatial, 76% at Besham Qila,92.9% at Shyok, 69.1% at Hunza, 47.9% at Gilgit and 57.0% at Astore tributary respectively. Conclusively, contrasting suspended sediment load variability was observed throughout the study area. Results indicate that serious soil erosion occurred mainly during three months (June, July and August). It is therefore, strongly recommended to reduce soil loss and launch soil conservating activities such as: toenhance vegetation cover,forestation and, professional development works in the area, which could play an effective role to extend the lifeline of proposed water resource projects, especially Tarbella (the largest reservoir), andthe Diamer Bhasha (an under-construction dam in the region).

Keywords*:* Suspended sediment load, Spatiotemporal variations, Factor analysis, Upper Indus basin, Pakistan.

Introduction

Estimation of suspended sediment load on seasonal and spatial scales plays a pivotal role in ecological and geomorphological assessment of the fluvial systems within a

catchment [1, 2], and the analysis of controlling factors of suspended sediment load (SSL), such as climatic factors (temperature and precipitation), land use changes, and river slope are very important to address the challenging issues like as soil erosion, pollutant transport, reservoir sedimentation and degradation of water quality and quantity [3-6]. The characteristics of SSL reflect the measurement of soil erosion, transport, and deposition in the river basin [7]. At the same time, the water quantity and quality of the freshwater bodies interact with the suspended sediments [8], which results in adverse impacts on the hydraulic structures and the aquatic environmental conditions [9]. The reservoirs of the dams, navigation waterways and barrages could be rendered unfeasible due to the accumulation of suspended sediments [10] and the maintenance of these structures may require dredging, with a significant cost from the management perspective [11]. Thus, the regular quantitative characterization of the suspended sediment load is crucial to cater for the existing research gap [12].

The Tibetan Plateau rightly known as the "Asian water tower" [13], plays a key role in feeding source of the Asian major rivers e.g., the Yangtze, Yellow, Indus, Brahmaputra and Ganges rivers, which supply fresh water to hundreds of millions population in surroundings and neighboring countries. Simultaneously, these rivers are also a major source of sediment transport to the oceans [14]. It is estimated that about one-third of the world's sediments entering the ocean come from rivers originating from the Third Pole Region [15]. Among these rivers, the river Indus is one of the highest sediment load transporters [16, 17], and it is the principal river of Pakistan [18].

Therefore, understanding the seasonal variation and spatial distribution of suspended sediment load and their controlling factors is very crucial for the sustainable development of water resources in the basin. However, as compared to the importance of the upper Indus basin, relatively fewer studies are available [19], which reflects a significant research gap on a regional scale, and such studies are not enough for the detailed explanation of the spatial differences of suspended sediment load.

The aim of this study is to provide detailed information on the seasonal and spatial distribution of suspended sediment load, and analysis of their controlling mechanisms in the upper Indus Basin, Pakistan. The outcomes of this study could assist in the identification of critical areas of soil erosion, determine the features of sediment transport and the sustainable management of the local water resources in the region, and could provide the foundations for soil and water conservation activities in the basin.

Materials and Methods

Study Area

The upper Indus basin (UIB), Pakistan, is selected for this study, the area comprises diverse physio-geographical features such as: complex Hindukush–Karakoram–Himalaya territory.

The study area extends from $72^0$03′-$77^0$44′ E and $34^0$16′-$37^0$06′ N (Fig. 1a) lying upstream of the Tarbella Dam and elongated between the western Himalaya and the Karakoram, with a length of 1125 km and with a drainage area of 219,830 km^2. The elevation of this area varies from 254 to 8570 m [20].

For a better explanation of the seasonal variation and spatial distribution of the suspended sediment load, the study area is further sub-divided into four stretches on the

basis of mainstream hydrological gauging stations such as Stretch-I from Kharmong to Kachura, Stretch-II from Kachura to BunjiBridge, Stretch-III from Bunji Bridge to Besham Qila and Stretch-IV from Besham Qila to Tarbella Outlet (upstream to the downstream direction).

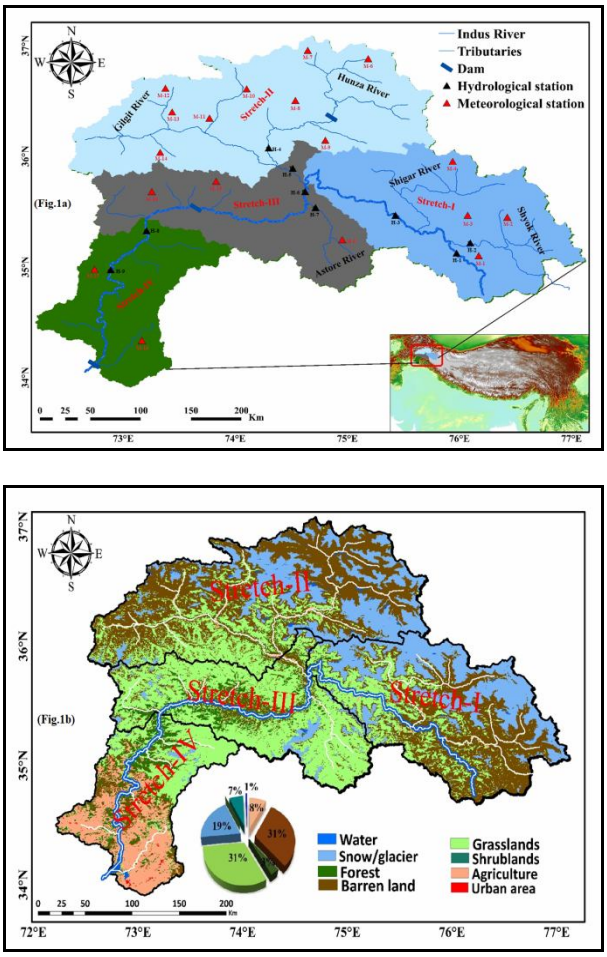

Figure 1. **(a) Location map of the upper Indus basin, Pakistan, four stretches, 9 hydrological stations (H-1 to H-9) including Indus mainstream and major tributaries Shyok, Hunza, Gilgit and Astore (Table A-1), and 18 meteorological stations (M-1 to M-18) (Table A-2) of the study area. (b) Land-use map of four stretches of the upper Indus River basin, Pakistan.**

Geology

The upper Indus basin (UIB), Pakistan demonstrates an excellent geological cross-section in the tectonic activities [21], the Himalayan orogeny during the mid-Eocene, and complex geological structures observed in the region [22].Due to extreme ruggedness and high altitudes, these young mountain ranges are subject to remarkably rapid degradation by a combined effect of weathering, erosion, and transportation [23]. Stretch-I, Stretch-II, and Stretch-III comprise the carbonates and silicates such as cherts, marbles, granites, limestones, dolomites and amphibolites[24], as well as metamorphic rocks such as greenschist and slate, tonalite, diorite, granite, gneiss, granodiorite, and hornblende-rich amphibolite, Pyrite and other sulfide minerals [25], and the Stretch- IV consist carbonates and silicates, including shales and quartzite, schists, gneisses, and granites with mafic intrusion and hydrothermal fluid deposits in the dikes [26].

Climate

The climate of the study area is representative of the South Asian Atmospheric Circulation strongly associated with the monsoon and extra-tropical cyclonic/anticyclonic circulations. The annual mean temperature of the area is -0.5 to 27.5 °C and the annual average precipitation is around 100 to 1200 mm. Precipitation in the UIB is largely controlled by the summer monsoon manipulating from the Indian Ocean, Bay of Bengal and Arabian Sea during July–September [27] and the western disturbances from the Mediterranean and the Caspian Sea as an extratropical frontal system during winter and early spring [28].

Land-use

The land-usein the study area is characterized into 8 major classes i.e., grasslands 30.5%, barren land 32.7%, glaciers/snow 21.4%, agriculture 3.8%, Shrubland 8.6%, forests 4.2%, residential 0.6%, and water 0.4. Data on land-use was extracted from the United States Geological Survey (USGS) land-use data (2010)

(Fig. 1b). The Stretch-I and II comprise highly elevated barren and glaciated areas, whereas, forest and grasslands are dominated in Stretch-III and Stretch-IV and the agricultural activities are primarily in Stretch-IV.

Whereas the major land-use types in the tributaries are barren lands, glacier-covered areas and grasslands (Fig. 1b). The glacier-covered area is dominated in upper tributaries Hunza and Shyok with 47% and 34%, respectively and the Gilgit and Astore are located in a relatively low glaciated area with 18.12 and 10.40%, respectively.

Data Collection

Due to limited data availability, eight years of hydro-meteorological data set i.e., daily temperature, precipitation, discharge, and weekly/biweekly SSC data during the period 2005-2012 were used in this study. Hydro-meteorological data from 9 hydrological and 18 meteorological stations were obtained from the Water and Power Development Authority (WAPDA) and Pakistan Meteorological Department (PMD). Those organizations are national level governmental agencies which are solely responsible for recording the synoptic hydro-meteorological variables, by following the standard operating procedures (SOPs) related to the installation of instruments and acquisition and dissemination of data to end users. Furthermore, the PMD is a member of the World Meteorological Organization (WMO). The hydrological variables such as discharge was measured with Price type AA current meters and the suspended sediment concentration was measured by following the standard USGS procedures [29, 30]. For the Gilgit basin, the hydrological data from Alam Bridge was used by subtracting the discharge, SSC values and drainage area of Hunza at Dainyor station to get the exact values for the Gilgit basin. Meteorological data from different stations were used to get an average temperature and precipitation in each Stretch. Locations of hydro-meteorological stations used in the current study are shown in (Fig.1a).

Data Analysis

Monthly and annual values of suspended sediment load and discharge were calculated from the daily data by using the following equations:

$$Q = \sum_{i=1}^{N}\sum_{j=1}^{M}\frac{q_{ij}t}{N} \quad (1)$$

$$SL = \sum_{i=1}^{N}\sum_{j=1}^{M}\frac{SSC_{ij}q_{ij}t}{N} \quad (2)$$

$$Q = \sum_{i=1}^{N}\sum_{j=1}^{M}\frac{q_{ij}t}{NSL} = \sum_{i=1}^{N}\sum_{j=1}^{M}\frac{SSC_{ij}q_{ij}t}{N}$$

where Q (V) and SL (M) are the average monthly and annual discharge and suspended sediment load, observed at a gauging station; q_{ij} (V/T) and SSC_{ij} (M/V) are the daily or weekly values of Q and SSC; t (T) represents the time period; and M represents the number of days in one month or one year while N shows the number of total years (8 years). Runoff depth (R, (L) and specific sediment yield (SSY, (M/A) were used as comparable variables by dividing the relative stretch area and calculated as follows:

$$R = \frac{Q_{i+1} - Q_i}{A_{i+1} - A_i} \quad (3)$$

$$SSY = \frac{SL_{i+1} - SL_i}{A_{i+1} - A_i} \quad (4)$$

where R (L) represents the runoff depth and SSY (M/A) is the specific sediment yield of a stretch between two gauging stations in a given period, A is the drainage area above a

given gauging station, and i represent the number of the gauging stations.

Hysteresis Curve Method

Quantifying the suspended sediment load in mountainous basins remains challenging in geomorphological research due to complexity of multisphere interactions and data scarcity [31]. As an alternative, empirical approaches are widely applied [32]. Hysteresis curve analysis is a widely used technique for identifying the sediment source areas or different processes in a basin, and hysteresis types based on the shape of discharge-sediment hysteresis loops[33]. The proximity of the sediment source and whether or not sediment depletion is occurring can be indicated by examining the temporal relationship between the discharge and suspended sediment peaks[33-35]. In this study, hysteresis curve method was applied to fit the inconsistent data and describe the relationship between discharge and SSC at four mainstream hydrological stations and four major tributaries of the study area.

Results and Discussions

In this section, the seasonal variation and spatial distribution of discharge and suspended sediment load and their major controlling factors are analyzed. The main impact factors including temperature, precipitation, land-use, river morphology and their impact mechanisms on the seasonal and spatial characteristics of sediment load are addressed.

Seasonal Variations of Discharge and Suspended Sediment Load

The high values of sediment loads were observed during the summer season, accounting for 77.4%, 85.6%, 73.7% and 76% at four mainstream stations and 92.9%, 69.1%, 47.9% and 57.0% at four major tributaries respectively. Peak sediment loads at mainstream stations occurred during June, July and August, and during July and August at major tributaries. This indicates that serious soil erosion occurred during these two months in the area. Significantly high values of SSC 1.41 kg/m^3 and SL 86.66 Mt are observed at Bunji Bridge. followed by Shatial, Kharmong and Besham. Moreover, the UIB is a glacier fed basin [36], and contributes more than 40%, considered as the major component of the discharge in the basin [37, 38]. Therefore, due to increase in temperature, May to September is considered the peak flow months, October to November is considered as the months of moderate flow, and December to next April is considered as the base flow season (Fig. 2 and Fig. 3). For further explanation, the seasons of the UIB are classified as winter (JFM), spring (AMJ), summer (JAS) and autumn (OND), and the seasonal comparison of four mainstream stations and four stations from major tributaries are briefly discussed below:

Comparison of four mainstream cross sections

The monthly discharge and sediment load at the four mainstream stations are plotted in Fig. 2. The upstream Kachura station is affected by the westerly winds, with more precipitation in winter and spring, and less than 20% in summer. However, the summer season is the period of high runoff and sediment transport, which concentrates on annual runoff and sediment transport and accounted for 63% and 77.4%, due to the impact of high temperature in summer which causes glaciers and snowmelt runoff, studies reported that the proportion of snowmelt in the region is 50 % as a fraction of total annual discharge, and 26% of total discharge is generated by the glacier melt in the region [39]. In the 2nd quarter (April-June), the runoff

and sediment transport were relatively high and accounted for 24.2% and 20.4% of the total of the whole year (Fig. 2). During the analysis of seasonal distribution, the month of June showed high discharge and suspended sediment concentration, however, the precipitation in June is not so high whereas the precipitation in April and May is relatively high but the discharge and suspended sediment is slightly low, the reason could be the solid precipitation due to the high altitude in the region. As the temperature increases, the snow starts to melt and becomes the main source of runoff in June and could cause the main driving force of sediment transport.

The Bunji Bridge station showed the combined impact of the westerlies and monsoon. Although, both are reaching a weak position in this area, therefore, it showed very low precipitation (177 mm), which mainly occurs in the 2nd and 3rd quarters, followed by the 1st quarter. The runoff and sediment transport significantly increased during the 2nd quarter especially from the month of May (although the precipitation during this month is very low) but mainly due to an increase in temperature which causes glacier melt in upstream areas of Kachura, Gilgit and Hunza basin and showed a very high concentration of discharge and suspended sediment during the 3rd quarter and accounting for 60.2% and 85.6% of the total (Fig. 2).

The downstream stations (Shatial and Besham Qila) both showed the strong impact of monsoon and reflected high precipitation during the summer season accounting for 31.9% and 42.8% of the annual precipitation, respectively. The precipitation in late monsoon (4th quarter) also increased, however, due to higher temperatures in the 2nd quarter, runoff and sediment transport accounted for a large proportion accounting for 23%-30% of the total annual volume and summer runoff accounted for nearly 60%, and sediment transport accounted for 75% approximately.

In general, the solid precipitation at high altitudes of the basin is the major contributor of runoff during the spring melt period and it could be the main driving source of sediment transport. The high temperature in summer leads to the increase of glacial meltwater runoff and the superposition of rainfall is characteristic of flood peak flow during the 2nd and 3rd quarter and the hydrological contribution of the 1st and 4th quarter is relatively low.

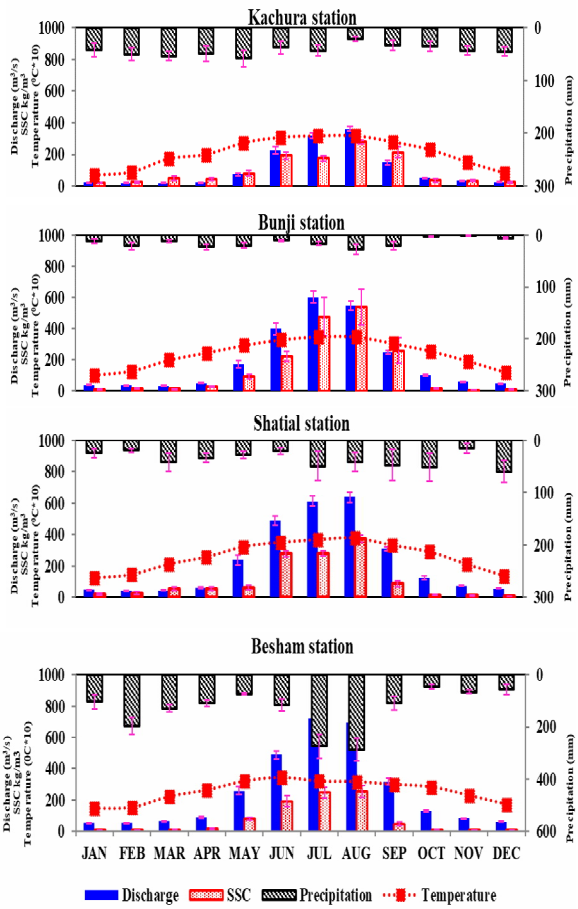

Figure 2. **Mean monthly distribution of discharge (m^3/s), suspended sediment concentration (SSC) (kg/m^3), precipitation (mm) and mean temperature ($^0C*10$) from 2005 to 2012 at four mainstream stations of the study area.**

Comparison of four main *tributaries*

The seasonal variations of discharge and suspended sediment load at the four main

tributaries are plotted in Fig. 3. At major tributaries, the effects of westerlies and monsoon are also significantly different in the distribution of rainfall during the year, and the seasonal distribution of runoff and sediment is also different. The Shyok River is located in the westerlies affected area with high altitude. The solid precipitation in winter and spring is larger, but due to the lower temperature, the amount of water in winter and spring is smaller. The runoff and sediment transport are highly concentrated in the summer season, accounting for 72% and 92.9% of the total of the whole year.

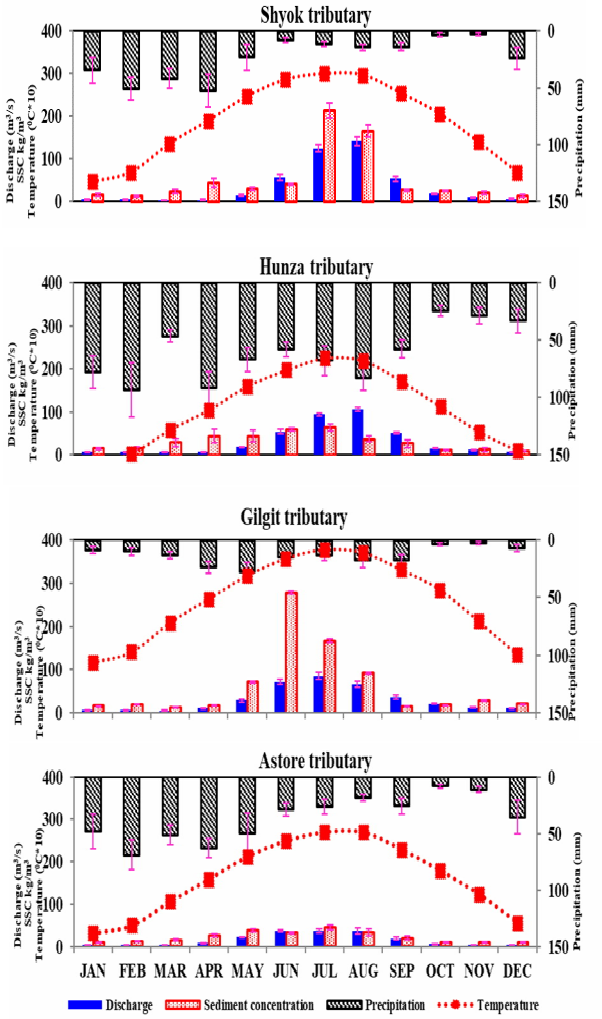

Figure 3. **Mean monthly distribution of discharge (m^3/s), suspended sediment concentration (SSC) (kg/m^3), precipitation (mm) and mean temperature ($^0C*10$) from 2005 to 2012 at four stations from major tributaries of the study area**

Although the rainfall distribution is slightly different in the other three tributaries, the runoff and sediment transport showed a higher proportion in the second quarter, which was significantly higher than the results of the four stations in the mainstream. And during the three months of the second quarter, the runoff increased significantly in June but the sediment showed high concentration throughout the quarter. And the Hunza, Gilgit, and Astore watersheds showed high concentration during the second quarter. The annual total runoff was 20.8%, 30.2%, and 36.1% respectively. The sediment transport accounted for 26.4%, 49.1%, and 38.5% of the annual sediment transport. Therefore, the effects of spring water melt on the soil erosion of these three tributaries cannot be ignored (Fig. 3).

Spatial Distribution of Discharge and Suspended Sediment Load

Comparison of four mainstream cross sections

The spatial distribution of discharge and suspended sediment load represent the total discharge and suspended sediment outflow of a basin during a specified time span. Discharge showed a significantly increasing trend at mainstream stations from the upstream to the downstream direction. And the sediment load showed a significant increase at upper stations and a decrease at lower stations. Moreover, as the catchment area increases, the runoff gradually increases. Annual runoff of the four mainstream stations is accounted for 349.1, 613.2, 717 and 789.9 (10^8 m^3), respectively. The sediment load significantly increases from Kachura to Bunji Bridge, and the maximum amount of sediment is observed at Bunji Bridge station, after that, it showed a decreasing trend at downstream stations (Shatial and Besham Qila). Annual sediment load at four mainstream stations accounted for 34, 86.66, 75.71 and 57.69 (Mt),

respectively (Fig. 4a). In order to better explanation of the spatial distribution of water and suspended sediment in different rivers in the upper and lower reaches, the river is sub-divided into four river sections (stretches), and the four tributaries are separately analyzed, using comparable indicators: such as SSC, Runoff depth, SSY, Runoff coefficient, etc.,

Comparison of four stretches

Runoff depth and runoff coefficient were calculated by removing the depth of the runoff and the sediment transport modulus (Fig. 4b). The runoff depth increases gradually from Stretch-I to Stretch-III and significantly decreases at Stretch-IV. As mentioned earlier the Stretch-IV is located at downstream, and due to the monsoon effect the average precipitation in the area is very high in comparison to other stretches, and reaching 1563 mm, but the runoff depth is only 599.1 mm, there could be two possible reasons: first, the glaciers in the area are relatively less than the other three stretches, which lacking the recharge contribution of glacial meltwater in the area and resulting in a lower runoff than the other three stretches; second, the increased water consumption, due to the dense vegetation cover, irrigation and domestic purposes in the region.

In order to further understand the spatial difference of runoff depth, the runoff coefficient α (Runoff coefficient) is calculated, and its values reflect the natural geographical features of the region and utilization of the water resources. Usually, the alpha value varies between 0 to 1, and its values are higher in wet areas and lower in arid areas. The alpha values of the first three stretches are greater than 1, which showed a typical feature of the glacial recharge in the basin. Generally, the larger values showed a greater proportion of glacial meltwater recharge. Such as the glacial area of Stretch-I and Stretch-II is relatively large. But the Stretch-I showed lower alpha values than Stretch-II due to highly elevated glacial areas and lower temperature. Whereas the Stretch-II shower higher alpha values than the other three stretches due to a larger glacial area and increased temperature. In addition, the runoff depth of stretch-II is less than stretch-III, but its alpha value is higher than Stretch-III. This could be due to larger glacial area in Stretch-II (Fig. 4b). Considering the proportion of water consumption in the underlying surface of the area, assuming that the integrated runoff coefficient generated by the three stretches of the upstream is ~2.22, 1.26~1.56 times, further estimate that the contribution rate of glacial meltwater in the total runoff of three stretches is: 30.6~42.6%, 65.8~69%, 55.7~60.9%. Whereas Stretch-IV showed its runoff coefficient 0.4~0.7, it can be estimated that the glacial meltwater runoff of this Stretch is 0.44~0.74. The reason for higher values of runoff-depth in Stretch-III could be the combined impact of glacial melt runoff from upper stretches and monsoon in the region because Stretch-III is located at the foothills of the upper high elevated and highly glaciated stretches of the basin (Fig. 4b). Moreover, increase or decrease in runoff depth is strongly depend on the morphometric characteristics of the slopes, lithology, land-use, rainfall patterns, soil and vegetation types of the area. Inconsistent patterns of runoff generation in the catchments are characterized by a flux discontinuity due to a hydrological disconnection between the elements of the slope. The slopes play a key role, like a mosaic of runoff and run-on areas [40].

Suspended sediment concentration and specific sediment yield were calculated from four stretches of the UIB (Fig. 4c). Results of SSY revealed that the area of Stretch-II is experiencing high erosion and it is the largest sediment transporter in the whole basin, and the SSY of Stretch-III and stretch-IV showed

negative values which reflect strong deposition, and accounted for 12.6% and 23.8% sediment deposition of the sediment transport volume at the respective upstream sites. The main reason for that deposition could be the gentle slope of the river bed. Slope gradients of the four river stretches are calculated as 2.1, 7.1, 2.2, and 3.0, respectively. Obviously, the channel slows down significantly from Stretch-II to Stretch-III and stretch-IV. This supports the high deposition in Stretch-III and stretch-IV regions. The deposition may cause riverbed elevation, siltation problems, and bring potential risk to regional flood control, water conservation projects and especially for the proposed Diamer Bhasha dam in the region. The average of suspended sediment concentration also indicates that the stretch-II is the highest sediment contributor and the SSC gradually decreases toward downstream at stretch-III and at stretch-IV, mainly due to the gentle river slope and improved vegetation cover in the area (Fig. 4c).

Comparison of four main tributaries

Figure 4d compares the runoff depth and runoff coefficient at the four tributaries. Runoff depth at four tributaries is Astore>Hunza>Gilgit>Shyok from higher to lower, showing an increasing trend from upstream to downstream. The value of the runoff coefficient α of the Shyok, Hunza, Gilgit, and Astore tributaries is greater than 1 such as 1.11, 2.52, 2.09, and 2.18, respectively. According to runoff values, the glacial area of the Hunza basin is larger than other sub-basins and the ratio of glacial meltwater runoff estimated by the coefficient is about 64.5~67.9%; the runoff coefficient of Gilgit and Astore basins and the proportion of glacial meltwater are similar, and the glacial runoff contribution ratio is between 58~64%, which is lower than that of the Hunza basin.

Whereas, the glacial area of the Shyok is relatively large, but the value of the runoff coefficient is not very high, which may be due to its higher altitude, lower temperature and lower melting rate in the region.

Suspended sediment concentration (SSC)and specific sediment yield were calculated from four tributaries of the basin (Fig. 4e). Results showed that the Shyok and Gilgit rivers are the largest sediment contributors to the mainstream followed by the Hunza and Astore river. However, the SSY calculated by removing the influence of the watershed area is Gilgit> Astore>Hunza>Shyok from higher to lower, indicating that the Gilgit River is the most severely eroded area in comparison to the other three tributaries. Similarly, the values of (SSC)at Gilgit are also very high, followed by the Shyok, Hunza, and Astore rivers (Fig. 4e). Moreover, the SSY, SL, and SSC of the Gilgit are very high which are confirming that the Gilgit is experiencing severe erosion and contributing a significant number of sediments to the mainstream. The glacial area of the Hunza basin is larger than the Gilgit but rainfall, runoff, and runoff coefficients of both basins are same. Whereas, the sediment concentration and sediment transport modulus of the Hunza basin is relatively low. This may be due to the development of the Atta Abad dam on the mainstream of the Hunza basin, which traps enough amount of suspended sediment. Moreover, the Shyok river has a large drainage area and a large sediment concentration, so it also contributes a significant amount of suspended sediment to the mainstream, but the erosion modulus of the basin shows very low values. Whereas, the Astore river is located in the lower part of the area, with better surface vegetation and lower sediment concentration. However, due to higher values of total water volume, the sediment transport modulus is roughly similar to that of Shyok and Hunza tributaries.

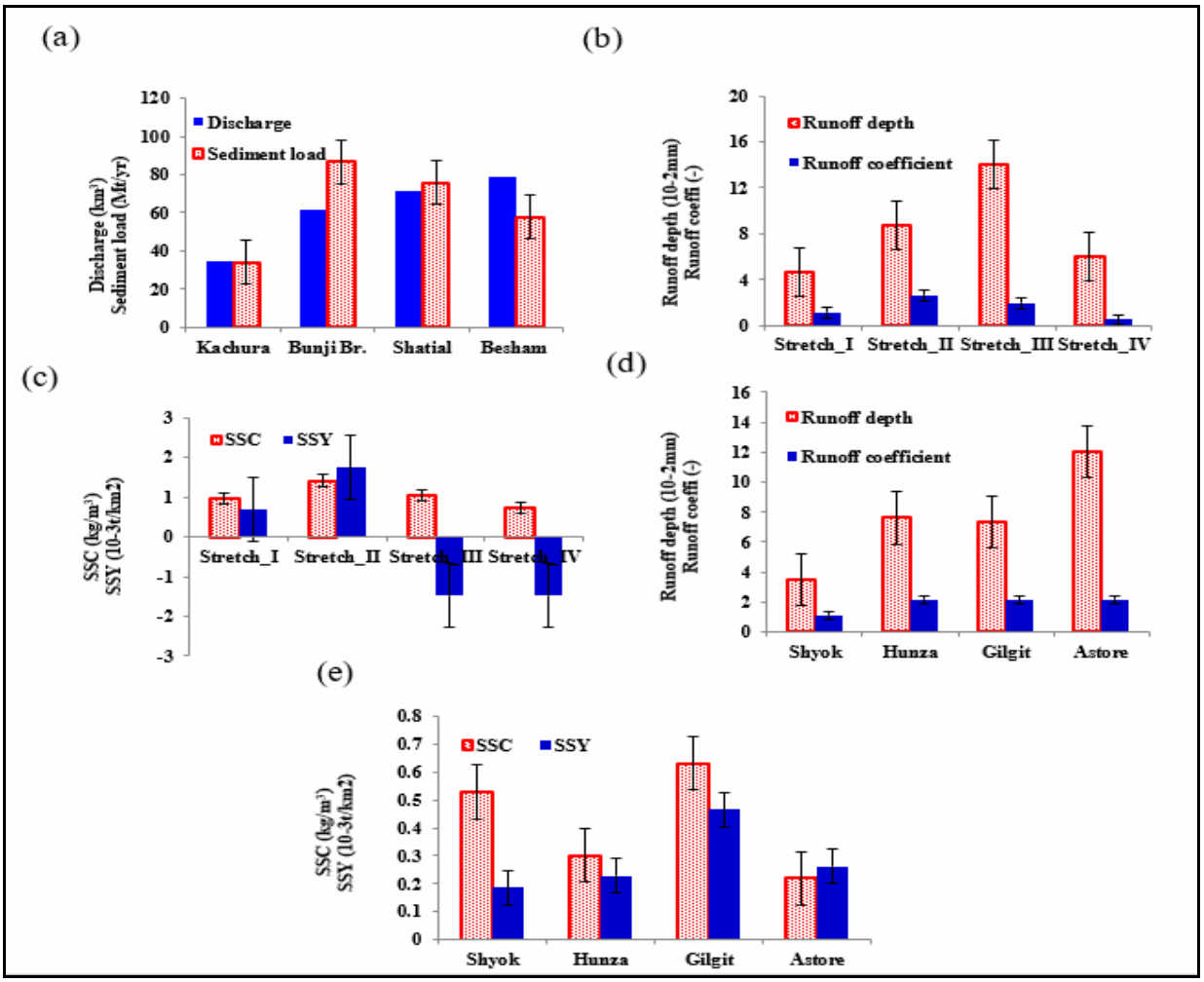

Figure 4. **(a) Annual runoff ($10^8 m^3$) and sediment load (Mt) at mainstream of the Indus river; (b) annual runoff depth (mm) and runoff coefficient (-) of four stretches; (c) annual suspended sediment concentration (SSC) (kg/m^3) and specific sediment yield (SSY) (t/km^2) of four stretches; (d) annual runoff depth (mm) and runoff coefficient (-) of four tributaries and (e) annual suspended sediment concentration (SSC) (kg/m^3) and specific sediment yield (SSY) (t/km^2) of four tributaries of the upper Indus basin, Pakistan.**

Hysteresis analysis between discharge and sediment

The hysteresis curves at four mainstream stations (Fig. 5) follow the "figure eight" patterns, which reflect the regional erosion processes are complex and sediment supplies may be from multiple sources. The conclusion seems to be reasonable because the mainstream receives multiple water sources from different tributaries which have different contribution rates of runoff supplies. Moreover, the patterns at the two lower stations are a little bit closer to a linear trend. That may be due to the large deposition of sediment above the stations which cause the curve patterns are fine-particle dominant.

To further understand the mechanism, the hysteresis curves at four tributaries are plotted in Fig. 5. In Shyok tributary, the relationship between discharge and SSC shows a two-segment linear pattern, i.e., stage of high discharge and high SSC between June and September and stage of low discharge and low SSC in other months. The linear pattern, where peaks of both discharge and SSC occur at the same time, implies a sediment source at an intermediate distance, a continuous supply of sediment or a lower entrainment threshold.

According to the above results, the Shyok tributary showed low runoff depth and high SSC, especially in the summer season and accounted for (92.9%). So, the linear pattern of hysteresis curve signifies that the sediment supply of Shyok tributary is relatively sufficient and easy to erode. As long as the floods are superimposed by summer meltwater and rainfall coming, a large amount of sediment can be eroded and transported, resulting in a high peak of SSC in the river.

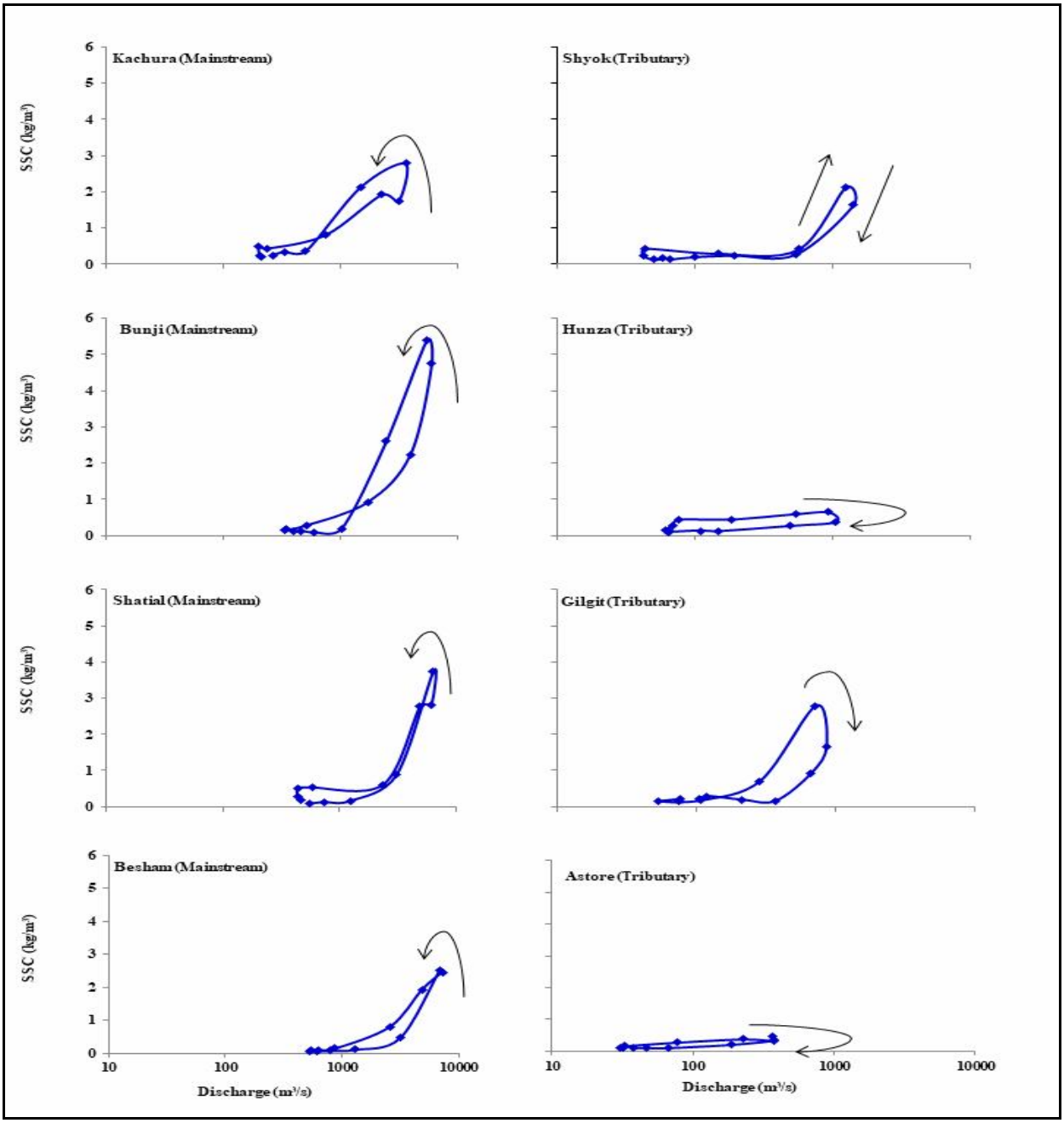

Figure 5. **Hysteresis curves between monthly mean SSC (kg/m^3), and discharge (m^3/s) at mainstream stations and major tributaries during the period 2005-2012**

The hysteresis curves in Hunza and Gilgit tributaries follows the clockwise patterns. Clockwise patterns represent the suspended sediment peaks that occur before discharge peaks, indicating a localized sediment source availability. The depletion of sediment sources is especially obvious in the Gilgit tributary. As shown in Fig. 5, during the period of the rain flood season, a smaller fluctuation of water discharge is corresponding to a larger fluctuation of SSC. In the rising stage (from May to July), the SSC first increase rapidly and then declines rapidly as well. Whereas, the runoff peak appearing in July and the SSC peak appearing in June. In the falling stage, the SSC decreases rapidly with the decrease of runoff, this illustrates that the Gilgit tributary should belong to either sediment supply limited (overall lack of sediment source) or relatively supply limited (more distant sediment source or a single source). According to the previous results, the Gilgit river is a tributary with high SSC and high SSY. The supply-limited is likely relative, which means that the sediment in the rain-flood period comes from the long distant glaciated area where the runoff fraction of glacier melt may be sediment supply limited while the local sediment supply is relatively sufficient for rainfall erosion. This deduction needs to be confirmed using field observations or model simulations in further study.

Hunza basin is adjacent to Gilgit tributary and has similar meteorological, hydrological and geographical conditions. In addition, the Hunza has the largest proportion of glacier covered area and the highest runoff coefficient. However, its sediment content is very low, and the difference between the rising and falling stage is very lower. Hunza River has the largest sediment load around the four tributaries by using early data. It means the Hunza river used to be a river of high sediment load. But in recent years, after the construction of Atta Abad dam, the sediment load has decreased significantly and consequently, the relationship between discharge and SSC is greatly affected by the dam capture and buffer function.

The hysteresis curve in Astore tributary follows the clockwise and linear approaching pattern, which reflects the sediment source is from a local or intermediate distance, i.e., from the lowlands but not from the glacier area. Although the tributary has the largest runoff depth, the SSC is relatively low, which may attribute to good surface land cover, which may reduce the surface sediment erosion of the region (Fig. 5).

Discharge and suspended sediment concentration

The mean annual discharge of the UIB, gradually increases from upstream to downstream direction. Annual runoff at four mainstream stations accounted for 349.1, 613.2, 717 and 789.9 ($10^8 m^3$), respectively. To show the annual pattern of discharge and SSC, a daily hydrograph is represented at the Besham Qila station (Fig. 6), which roughly showed a similar pattern of the discharge and suspended sediment concentration, except 2010, which is the year of super flood in the region.

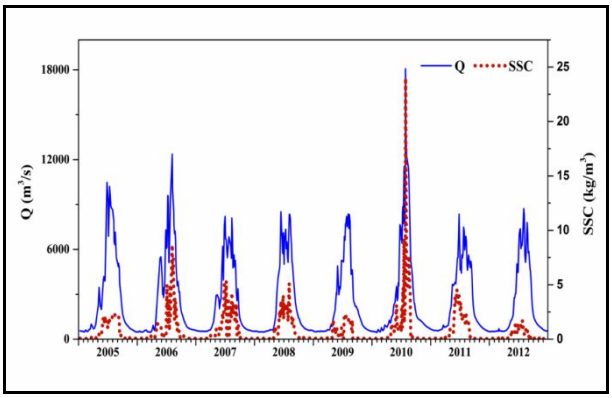

Figure 6. **The hydrograph with sediment concentrations SSC (kg/m^3) and discharge (m^3/s) at Besham Qila (Stretch-IV) from January 2005 to December 2012**

Conclusions

Contrasting suspend sediment load variability was observed throughout the study area. The high values of sediment loads were observed during the summer season, accounting for 77.4%, 85.6%, 73.7% and 76% at four mainstream stations and 92.9%, 69.1%, 47.9% and 57.0% at four major tributaries respectively. Peak sediment loads at mainstream stations occurred during June, July and August, and during July and August at major tributaries. This indicate that serious soil erosion is occurred during these two months in the area.

The upper parts of the basin (Kachura, Yugo, Hunza and Gilgit) showed a strong impact of temperature, westerly winds, barren lands and steep slopes in the area, however, the middle parts (Bunji and Astore) reflect the combined impact of the westerlies and monsoon. Although, both are reaching a weak position in this area and the lower parts (Shatial and Besham) showed the combined impact of the discharge and sediment load from upstream areas and monsoon in the region.

In general, the area of Stretch- I and II is experiencing high erosion and considered as the largest sediment transporter in the whole basin, and the area of Stretch-III and IV showed negative values which reflect strong deposition. And according to the results of discharge and sediment budget, the discharge showed an increasing trend from upstream to downstream direction, whereas the sediment showed increasing trend from Stretch-1 to Stretch-II and decreasing trend from Stretch-III to Stretch-IV. And the results of SSY revealed that among the major tributaries, Shyok and Gilgit river are the largest sediment contributors to the mainstream followed by the Hunza and Astore river. It is therefore, soil conservating activities, forestation and professional development works are highly recommended to reduce soil erosion and transportation in the area, which could play an effective role to extend the lifeline of proposed water resource projects, especially the Diamer Bhasha (an under-construction dam in the region).

Acknowledgements

This research was financially supported by the Second Tibetan Plateau Scientific Expedition and Research (STEP) program (grant no. 2019QZKK0203) and the Chinese Academy of Sciences-The World Academy of Sciences (CAS-TWAS) President's Fellowship Program 2016 for Muhammad DodoJagirani's Ph.D study. The authors express their deepest gratitude to Water and Power Development Authority Pakistan (WAPDA) and Pakistan Meteorological Department (PMD) for sharing the hydro-meteorological data for this study. In addition, Muhammad Dodo Jagirani pays special thanks to the College Education Department, Government of Sindh, Pakistan for study leave to pursue the Ph.D. Degree.

Conflitc of Interest

All authors declear that, there is no conflict of interest.

References

1. W. Guo, X. Xu, T. Zhu, H. Zhang, W. Wang, Y. Liu and M. Zhu, *J. Soils Sed.*, 20 (2020) 1730. https://doi.org/10.1007/s11368-019-02496-z.
2. A. Rymszewicz, M. Bruen, J. O'Sullivan, J. Turner, D. Lawler, J. R. Harrington, E. Conroy and M. Kelly-Quinn, *Sci. Total Environ.*, 619 (2018) 672.

https://doi.org/10.1016/j.scitotenv.2017.10.134.
3. T. Li, S. Wang, Y. Liu, B. Fu and W. Zhao, *J. Soils Sed.*, 20 (2020) 1719. https://doi.org/10.1007/s11368-019-02495-0.
4. A. Bonometto, A. Feola, F. Rampazzo, C. Gion, D. Berto, E. Ponis and R. B. Brusà, *Sci. Total Environ.*, 650 (2019) 1832. https://doi.org/10.1016/j.scitotenv.2018.09.142.
5. W. Duan, K. Takara, B. He, P. Luo, D. Nover and Y. Yamashiki, *Sci. Total Environ.*, 461 (2013) 499. https://doi.org/10.1016/j.scitotenv.2013.05.022.
6. S. T. Harrington and J. R. Harrington, *Geomorphology*, 185 (2013) 27. https://doi.org/10.1016/j.geomorph.2012.12.002.
7. Z. Suif, A. Fleifle, C. Yoshimura and O. Saavedra, *Sci. Total Environ.*, 568 (2016) 933. https://doi.org/10.1016/j.scitotenv.2015.12.134.
8. G. Hancock, J. Hugo, A. Webb and L. Turner, *J. Hydrol.*, 547 (2017) 613. https://doi.org/10.1016/j.jhydrol.2017.02.022.
9. A. Yadav and P. Satyannarayana, *Int. J. River Basin Manag.*, 18 (2020) 207. https://doi.org/10.1080/15715124.2019.1705317.
10. M. Dietrich, K. B. Best, J. L. Raff and E. R. Ronay, *Sci. Total Environ.*, 726 (2020) 138667. https://doi.org/10.1016/j.scitotenv.2020.138667.
11. ICOLD, CIGB. "Sedimentation and sustainable use of reservoir and river systems." *Draft ICOLD. Bull. Sedimentation Committee*, (2009). https://www.scirp.org/(S(i43dyn45teexjx455qlt3d2q))/reference/ReferencesPapers.aspx?ReferenceID=2028666
12. E. Kellner and J. A. Hubbart, *Sci. Total Environ.*, 615 (2018) 1164. https://doi.org/10.1016/j.scitotenv.2017.10.040.
13. W. W. Immerzeel, L. P. Van Beek and M. F. Bierkens, *Science*, 328 (2010) 1382. https://doi.org/10.1126/science.1183188.
14. L. Cao, S. Liu, S. Wang, Q. Cheng, A.E. Fryar, L. Zhang, Z. Zhang, F. Yue, T. Peng, Journal of Hydrology; 594 (2021) 125792. https://doi.org/10.1016/j.jhydrol.2020.125792
15. X. Shi, F. Zhang, X. Lu, Z. Wang, T. Gong, G. Wang and H. Zhang, *Earth Surf. Process. Landforms.*, 43 (2018) 432. https://doi.org/10.1002/esp.4258.
16. K. F. Ali and D. H. De Boer, *J. Hydrol.*, 334 (2007) 368. https://doi.org/10.1016/j.jhydrol.2006.10.013.
17. D. Nag and B. Phartiyal, *Quat. Int.*, 371 (2015) 87. https://doi.org/10.1016/j.quaint.2014.08.045.
18. A. Khan, K. S. Richards, G. T. Parker, A. McRobie and B. Mukhopadhyay, *J. Hydrol.*, 509 (2014) 442. https://doi.org/10.1016/j.scitotenv.2016.01.001
19. M. A. Sabir, S. Shafiq-Ur-Rehman, M. Umar, A. Waseem, M. Farooq and A. R. Khan, *Pol. J. Environ. Stud.*, 22 (2013). https://doi.org/10.1134/S0097807814050091
20. Y. Latif, M. Yaoming and M. Yaseen, *Theor. Appl. Climatol.*, 131 (2018) 761. https://doi.org/10.1007/s00704-016-2007-3.
21. M. Searle, M. A. Khan, J. Fraser, S. Gough and M. Q. Jan, *Tectonics*, 18 (1999) 929. https://doi.org/10.1029/1999TC900042

22. K. J. Miller, *The International Karakoram Project: Volume 1*. (1984): Cambridge University Press. https://academic.oup.com/gji/article/79/3/1023/766664
23. J. F. Shroder Jr, *Himalaya to the sea: geology, geomorphology and the Quaternary*. (2002): Routledge. https://www.taylorfrancis.com/chapters/edit/10.4324/9780203414637-12/himalaya-sea-geomorphology-quaternary-pakistan-regional-context-john-shroder-jr
24. Y. Zou, X. Chen, W. Huang, J. Zhang, H. Liang, J. Xu and L. Chen, *Sci. Bull.*, 62 (2017) 888. https://doi.org/https://doi.org/10.1016/j.scib.2017.05.026.
25. C. Andrews-Speed and M. Brookfield, *Tectonophysics*, 82 (1982) 253. https://doi.org/10.1016/0040-1951(82)90048-8.
26. M. Petterson and B. Windley, *Earth Planet. Sci. Lett.*, 102 (1991) 326. https://doi.org/10.1016/0012-821X(91)90027-F.
27. Z. Ahmad, M. Hafeez and I. Ahmad, *Environ. Monit. Assess.*, 184 (2012) 5255. https://doi.org/10.1007/s10661-011-2337-7.
28. Z. H. Dahri, F. Ludwig, E. Moors, B. Ahmad, A. Khan and P. Kabat, *Sci. Total Environ.*, 548 (2016) 289. https://doi.org/10.1016/j.scitotenv.2016.01.001.
29. K. F. Ali, D. H. De Boer, *Water Resour. Res.*, 46 (2010). https://doi.org/10.1029/2009WR008762, 2010.
30. T. K. Edwards, G. D. Glysson and G. Survey, *Field Methods for Measurement of Fluvial Sediment*. (1999): U.S. Department of the Interior, U.S. Geological Survey. https://pubs.usgs.gov/twri/twri3-c2/
31. J. de Vente, J. Poesen, G. Verstraeten. *Evaluation of reservoir sedimentation as a methodology for sediment yield assessment in the Mediterranean: challenges and limitations*. in *SecondSCAPE Workshop, Cinque Terre, Italy*. (2004). https://www.researchgate.net/profile/Gert-Verstraeten/publication/242549491
32. M. Zheng, *Sci. Total Environ.*, 630 (2018) 1453. https://doi.org/10.1016/j.scitotenv.2018.02.323.
33. S. E. Martin, M. H. Conklin and R. C. Bales, *Water*, 6 (2014) 2144. https://doi.org/10.3390/w6072144.
34. G. P. Williams, *Water Resour. Res.*, 14 (1978) 1141. https://doi.org/10.1029/WR014i006p01141.
35. P. Wood, *Sedimentology*, 24 (1977) 437. https://doi.org/10.1111/j.1365-3091.1977.tb00131.x.
36. B. Mukhopadhyay and A. Khan, *J. Hydrol.*, 527 (2015) 119. https://doi.org/10.1016/j.jhydrol.2015.04.045.
37. A. Kääb, E. Berthier, C. Nuth, J. Gardelle and Y. Arnaud, *Nature*, 488 (2012) 495. https://doi.org/10.1038/nature11324.
38. J. M. Shea and W. W. Immerzeel, *Ann. Glaciol.*, 57 (2016) 308. https://doi.org/10.3189/2016aog71a073.
39. W.W. Immerzeel, F. Pellicciotti, A. B. Shrestha, *Mt. Res. Dev.*, 32 (2012) 30. https://doi.org/10.1659/mrd-journal-d-11-00097.1.
40. A. Calvo-Cases, C. Boix-Fayos and A. Imeson, *Geomorphology*, 50 (2003) 269. https://doi.org/10.1016/S0169-555X(02)00218-0.